# FOS Operation in the South Atlantic Anomaly

W. A. Baity, E. A. Beaver, J. B. Linsky and R. W. Lyons
*University of California, San Diego*

**FOS Instrument Science Report CAL/FOS-079**
May 1992

## Abstract

Operational boundaries defining the South Atlantic Anomaly (SAA), as determined from FOS OV 2748, are presented. The **normal contour**, corresponding to a measured background rate of **0.04 counts/sec/diode**, is very similar to the normal operational boundary that we previously determined for the GHRS. A low background contour, which corresponds to a rate of 0.02 counts/sec/diode has been established for special use when a particularly low background is required.

## I. Introduction

SAA testing for the FOS was first proposed prior to 1988 when the potential effects of the trapped radiation in the South Atlantic (Geomagnetic) Anomaly on HST instrumentation were not fully appreciated throughout the Project. As launch approached and it became evident that the Sun was more active than in any previous measured cycle, concern arose as to whether some or all of the Science Instruments (and possibly the HST fine guidance sensors) might have to be turned off during SAA passages. This would have had a large impact to the observing schedule. We initially used the GSFC provisional Launch Contour (#5) for the SAA, based on the work of Stassinopoulos some 20 years previously. We also had access to SAA data (Baity, unpublished) from the HEAO A-1 charged particle detectors in 1977 - 1979, during the previous solar maximum. Several changes to the test plan were made late in the planning process to check early for HV operability and later to reduce Blue side testing, given the success on the Red side and to accommodate a delay in Blue side availability.

The OV 2748 testing was initially planned for 10 passes through the SAA for each side of the FOS, moving along the orbit from West to East, with the first several orbits on successive days to allow plenty of time for analysis. Orbit types (see Table 1 below) were established, parameterized by the ascending node longitude (Omega), which allowed us to specify which tests were to be run in various regions of the SAA. Orbits on successive days cut progressively deeply into the SAA from skimming the eastern edge towards more central passages. The ground paths of the actual data takes for the Red Side are shown in Figure 1. The gaps are pauses to record data to the on-board tape recorders. There were calibration runs with the FOS cal lamps 15 minutes before and 10 minutes after each SAA passage.

**Table 1 -- SAA Orbit Type Definitions (9/26/88)**

| Type | # from last SAA | Asc. Node Longitude | Minutes in SAA | Comments |
|---|---|---|---|---|
| 10 | 15 - 9 | 23W - 175E | 0 | No usable SAA crossing |
| 9 | 8 | 174E - 155E | 5 - 22 | Skirts E edge of SAA |
| 8 | 7 | 154E - 133E | 22 - 25 | East SAA & high energy tail |
| 7 | 6 | 132E - 111E | 25 - 26 | Penetrates inner SAA |
| 6 | 5 | 110E - 89E | 26 - 27 | To core SAA |
| 5 | 4 | 88E - 67E | 27 - 25 | Longest core SAA |
| 4 | 3 | 66E - 45E | 25 - 23 | West to East through SAA |
| 3 | 2 | 44E - 23E | 22 - 19 | To West of core |
| 2 | 1 | 22E - 0 | 19 - 15 | Less exposure, W of core |
| 1 | Last | 0 - 22W | 15 - 5 | Skirts W edge of SAA |

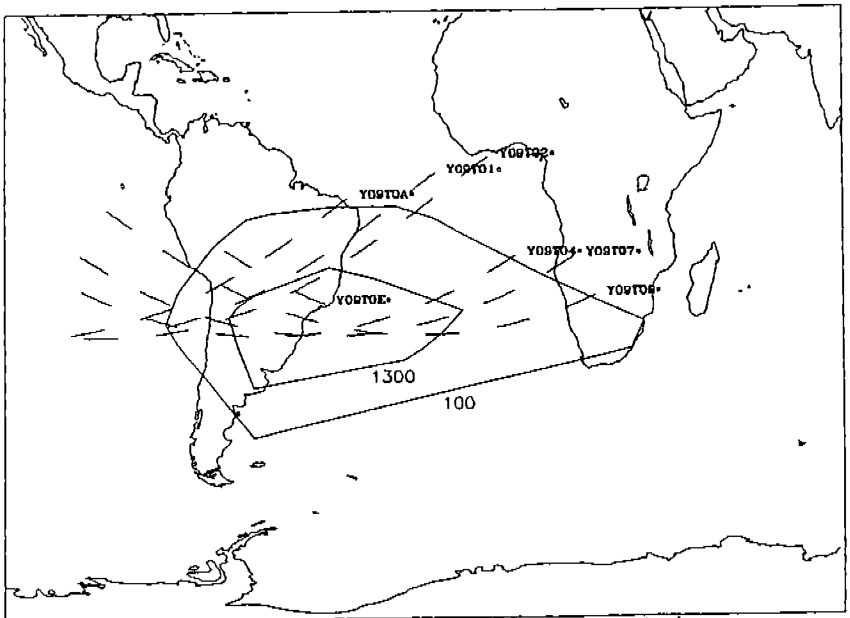


* SAA Contours for Solar Minimum, E 50 MeV (Stassinopoulos)
* fluxes in protons/cm^-2/sec

**Figure 1 -- Early Sampling of the SAA for FOS Survivability**

There were several purposes to these SAA tests:

1) Issues of health and safety, which needed to be evaluated quickly to permit the next day's test to proceed. Eventually we found that it was safe to leave high voltage (HV) on the FOS Digicons throughout the SAA during an observation run, and this policy was implemented very early in OV.

2) issues of optimal location of operational FOS boundaries for the SAA, addressed here and implemented in February, 1992 in the SVDF.DAT table at the STScI.

3) Issues on the use of FOS burst noise rejection software limits (REJLIM), addressed in the companion CAL/FOS-076. Further testing is recommended.

4) Issues of fluorescence in the FOS prism disperser, the effectiveness of the internal FOS baffles and the feasibility of performing FOS Target Acquisitions in the SAA, to improve the HST efficiency factor. These studies were curtailed in the reorganization of this test; the Target Acquisition test would have been difficult early in the mission in any case, due to the spherical aberration and jitter problems not being well understood.

In order to carry out these diverse objectives, SAA passes of the same general nature were to be repeated with different REJLIM settings and various optical elements such as gratings, prism and mirror. The original test sequence for each side is shown below.

**Table 2 -- Planned SAA Test Sequence**

| Day | Orbit Type | Disperser | Noise Reject | Shutter | Aperture | Notes |
|---|---|---|---|---|---|---|
| 1 | 1 | Prism | Off | Closed | N/A | Mapping SAA |
| 2 | 2 | Prism | Off | Closed | N/A | Mapping SAA |
| 2 | 1 | Prism | On | Closed | N/A | Noise Rejection |
| 3 | 3 | Prism | Off | Closed | N/A | Mapping SAA |
| 3 | 2 | G130H | On | Closed | N/A | Baffle Test |
| 3 | 1 | Mirror | On | Closed | N/A | Fluor. & T.A. |
| 4 | 4 | Prism | Off | Closed | N/A | Mapping SAA |
| 4 | 3 | G780H | On | Closed | N/A | Baffle Test |
| 4 | 2 | Mirror | On | Closed | N/A | Fluor. & T.A. |
| 4 | 1 | G650L | Off | Closed | N/A | Baffle Test |
| 5 | 5 | Prism | Off | Closed | N/A | Mapping SAA |
| 5 | 4 | Prism | On | Closed | N/A | Noise rejection |
| 5 | 3 | Mirror | On | Closed | N/A | Fluor. & T.A. |
| 6 | 6 | Mirror | Off | Open | 1.0 | Sky Background |
| 6 | 5 | G650L | On | Closed | N/A | Baffle Test |

## II. Data Analysis

Data taken for OV 2748 are summarized in Tables 3 and 4 below. Each pass through the SAA was assigned a distinctive data ID, of the form Y09T0w, where w is the run ID. F is the number of files (data takes) in a given pass. All data were taken with the B2, 0.3 arcsec circular aperture. Note that since the aperture door was closed, no light should have been coming through the optics.

**Table 3 -- Actual Red Digicon SAA Testing**

| Date | Start Time | F | Peak Counts | Data ID | Optics | Comments |
|---|---|---|---|---|---|---|
| 07/16/90 | 09:27 | 7 | 0.64 | 1 | Prism | |
| 07/20/90 | 06:55 | 9 | 0.66 | 2 | Prism | |
| 07/20/90 | 08:38 | 7 | 0 | 3 | Prism | REJLIM = 3 |
| 07/21/90 | 03:43 | 9 | 0.98 | 4 | Prism | |
| 07/21/90 | 05:26 | 9 | 0 | 5 | Prism | REJLIM = 17 |
| 07/21/90 | 07:09 | 7 | 0 | 6 | Prism | REJLIM = 3 |
| 07/22/90 | 02:14 | 10 | 1.24 | 7 | Prism | |
| 07/22/90 | 03:58 | 9 | 0 | 8 | Prism | REJLIM = 34 |
| 07/22/90 | 05:41 | 9 | 0 | 9 | Prism | REJLIM = 17 |
| 07/22/90 | 07:24 | 7 | 0.29 | A | G650L | |
| 07/26/90 | 22:19 | 10 | 1.07 | B | Prism | |
| 07/27/90 | 00:02 | 10 | 0 | C | Prism | REJLIM = 112 |
| 07/27/90 | 01:45 | 9 | 0 | D | Prism | REJLIM = 34 |
| 07/27/90 | 20:58 | 4 | 0.93 | E | Prism | |
| 07/27/90 | 22:34 | 10 | 0 | F | G650L | REJLIM = 112 |

**Table 4 -- Actual Blue Digicon SAA Testing**

| Date | Start Time | F | Peak Counts | Data ID | Optics | Comments |
|---|---|---|---|---|---|---|
| 10/01/90 | 15:10 | 8 | 0.55 | M | Prism | |
| 10/01/90 | 18:08 | 7 | 0.70 | J | Prism | |
| 10/01/90 | 19:51 | 7 | 0.25 | H | Prism | |
| 10/01/90 | 21:34 | 5 | 0.06 | G | Prism | |
| 10/03/90 | 16:53 | 6 | 0 | N | Prism | REJLIM = 34 |
| 10/03/90 | 18;36 | 6 | 0 | O | Prism | REJLIM = 17 |
| 10/03/90 | 20:19 | 5 | 0.08 | P | G650L | |
| 10/06/90 | 10:04 | 5 | 0.23 | T | Prism | |
| 10/06/90 | 14:10 | 8 | 0.70 | Q | Prism | |
| 10/06/90 | 15:53 | 8 | 0 | R | Prism | REJLIM = ? |

It became obvious that the charged particle-induced Cerenkov light generated inside the FOS Digicon faceplates was causing the rejection of many frames of data inside the SAA, even at the liberal limit of 112 counts in each 0.25 second frame. Use of the FOS microprocessor burst noise rejection software is very effective in eliminating background noise; see CAL/FOS-076 for further details. We are interested here in studying the "noise" to determine operational SAA boundaries.

## III. Selection of Operational Boundaries

The locations of data takes for the Red side are shown in Figure 1, together with the contour used as the standard pre-launch, based upon that published 20 years previously by Stassinopoulos for 10 protons/cm$^2$/sec with energies > 10 MeV or a flux of 1000 electrons/cm$^2$/sec with energies > 0.5 MeV.

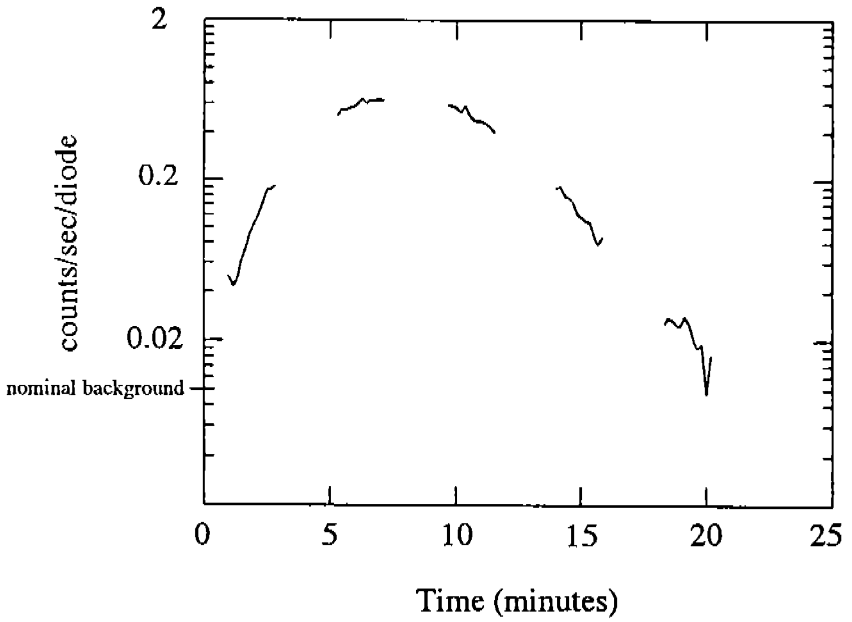


**Figure 2 -- Typical Count Rate in the SAA**

Figure 2 shows a typical count rate through the SAA, with data taken during 2 minute periods, shown with solid lines The blanks correspond to the 2 minute readout gaps. The times were noted and thus the latitudes and longitudes of the HST at the count rates to be used for contours were computed. This was done for the FOS Red detector only, as the Blue detector data did not adequately sample the SAA, although where we had overlapping data, the results looked similar for both detectors. The vertex points were linked and plotted out over a world map contained in an IDL utility. The location of any given point is only good to +/- 1 degree in either longitude or latitude. Where there was any doubt, the vertices were chosen conservatively, to give a bigger SAA.

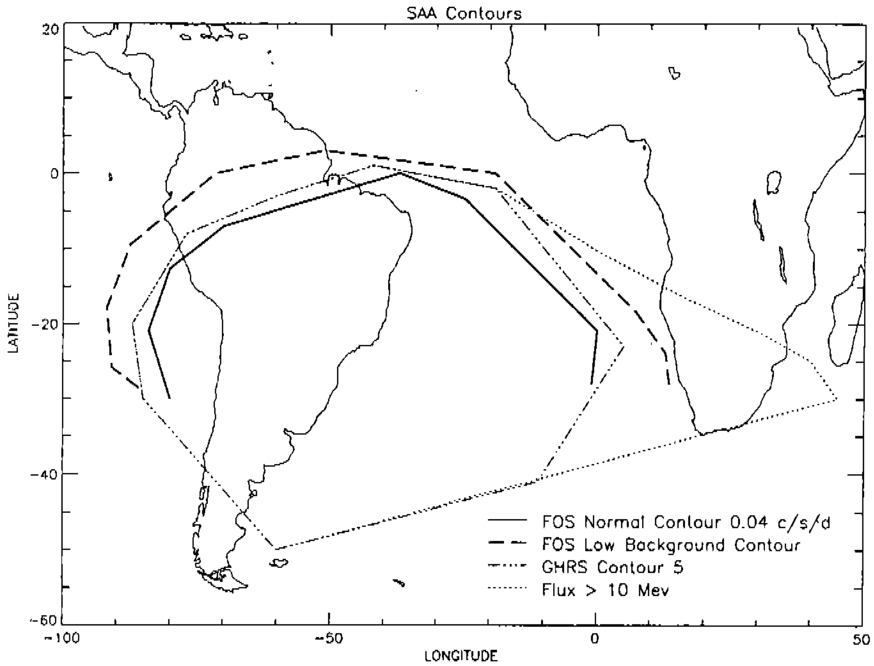


**Figure 3 -- FOS Operational Contours**

The resulting map is shown in Figure 3, which displays the outermost two contours of interest to the FOS at 0.02 and 0.04 counts/sec/diode, together with the GHRS 0.02 counts/sec/diode, which we had previously determined, modified at the STScI so as not to intersect the FOS contour. Also shown is the previous standard contour. These FOS contours are now resident on the STScI Project Data Base (PDB) file SAA Vertex Definition File (SVDF.DAT):

**Table 5 -- SVDF.DAT File Contents**

| FOS Normal, Contour 6 | | FOS Low Background, Contour 18 | |
|---|---|---|---|
| **Latitude** | **Longitude** | **Latitude** | **Longitude** |
| -28.0 | 359.0 | -28.0 | 013.5 |
| -20.9 | 360.0 | -23.9 | 012.8 |
| -03.4 | 335.4 | -18.3 | 007.2 |
| -00.0 | 323.0 | 00.0 | 341.0 |
| -07.0 | 290.0 | +3.0 | 309.0 |
| -12.6 | 280.0 | 00.0 | 288.5 |
| -20.9 | 276.0 | -9.4 | 272.6 |
| -30.0 | 280.0 | -17.8 | 268.2 |
| | | -25.8 | 269.1 |
| | | -29.0 | 275.0 |

There appears to be a slight shift of the maximum SAA count rates to the West , plus a lack of a marked Eastward tail over Africa, in the HST data relative to measurements taken years previously on other spacecraft.

## IV. Summary

It is safe to leave the FOS HV on during the SAA. Operational SAA contours for the FOS have been entered into the project data base (PDB). FOS burst noise rejection software was found effective (see CAL/FOS-076), and further testing on an astronomical object with REJLIM = 1 will be proposed. Further testing in the SAA might lead to improvements to the HST efficiency by establishing that some FOS target acquisitions and even certain observations might be carried out in the SAA, using time that is currently unused, thereby increasing HST efficiency.

## References


Beaver, E. A. and Lyons, R. W. "Analysis of FOS On-Orbit Detector Background with Burst Noise Rejection", *Instrument Science Report CAL/FOS-076,* April 1992.

Rosenblatt, E. I., Beaver, E.A., Linsky, J. B., Lyons, R. W., 1991 "Background Noise Rejection in the Faint Object Spectrograph", *The First Year of HST Observations*, ed. Kinney and Blades, pp. 234-237.

Rosenblatt, E. I., Beaver, E. A., Cohen, R. D., Linsky, J. B. and Lyons, R. W., 1991 *SPIE Proceedings on Electron Image Tubes and Image Intensifiers II*, ed. I. P. Csorba (Bellingham, WA: SPIE), **1449**, p. 72.

Stassinopoulos, E. G. and King, J. H. 1974 " Empirical Solar proton Model for Orbiting Spacecraft Applications", *IEEE Trans. AES*, **AES-10**, No. 4.